3-28-2022

Hydrogen flooding of a coal core: Effect on coal swelling

Stefan Iglauer
Edith Cowan University, s.iglauer@ecu.edu.au

Hamed Akhondzadeh
Edith Cowan University, h.akhondzadeh@ecu.edu.au

Hussein Abid
Edith Cowan University, h.alfatlawi@ecu.edu.au

Adriana Paluszny

Alireza Keshavarz
Edith Cowan University, a.keshavarz@ecu.edu.au

See next page for additional authors

Authors

Stefan Iglauer, Hamed Akhondzadeh, Hussein Abid, Adriana Paluszny, Alireza Keshavarz, Muhammad Ali, Ausama Giwelli, Lionel Esteban, Joel Sarout, and Maxim Lebedev

Hydrogen Flooding of a Coal Core: Effect on Coal Swelling

Stefan Iglauer[1] , Hamed Akhondzadeh[1], Hussein Abid[1] , Adriana Paluszny[2] , Alireza Keshavarz[1] , Muhammad Ali[3], Ausama Giwelli[4] , Lionel Esteban[4] , Joel Sarout[4] , and Maxim Lebedev[5]

[1]School of Engineering, Edith Cowan University, Joondalup, WA, Australia, [2]Department of Earth Science and Engineering, Imperial College London, London, UK, [3]Physical Science and Engineering Division, King Abdullah University of Science and Technology (KAUST), Thuwal, Saudi Arabia, [4]CSIRO Energy Business Unit, Kensington, WA, Australia, [5]Western Australian School of Mines (WASM): Minerals, Energy and Chemical Engineering, Curtin University, Kensington, WA, Australia

Abstract Hydrogen is a clean fuel which has the potential to drastically decarbonize the energy supply chain. However, hydrogen storage is currently a key challenge; one solution to this problem is hydrogen geo-storage, with which very large quantities of H_2 can be stored economically. Possible target formations are deep coal seams, and coal permeability is a key parameter which determines how fast H_2 can be injected and withdrawn again. However, it is well known that gas injection into coal can lead to coal swelling, which drastically reduces permeability. We thus injected H_2 gas into a coal core and measured dynamic permeability, while imaging the core via x-ray micro-tomography at reservoir conditions. Importantly, no changes in coal cleat morphology or permeability were observed. We conclude that H_2 geo-storage in deep coal seams is feasible from a fundamental petro-physical perspective; this work thus aids in the large-scale implementation of a hydrogen economy.

Plain Language Summary Hydrogen is a clean fuel which has the potential to drastically decarbonize the energy supply chain. However, hydrogen storage is currently a key challenge; one solution to this problem is hydrogen geo-storage, with which very large quantities of H_2 can be stored economically. Earlier it has been shown that coal can adsorb and thus storage large quantities of hydrogen. Here we now demonstrate experimentally that coal permeability (and thus hydrogen injectivity and withdrawal capacity) is not affected by hydrogen flooding. We conclude that H_2 geo-storage in deep coal seams is feasible from a fundamental petro-physical perspective; this work thus aids in the large-scale implementation of a hydrogen economy.

1. Introduction

Hydrogen is a clean fuel which has the potential to completely decarbonize the energy supply chain (e.g., compare Hanley et al., 2018; Tarkowski, 2019). Hydrogen is currently stored in high-pressure surface tanks or in chemical form (e.g., as ammonium or hydride, Berta et al., 2018; F. Zhang, Zhao, et al., 2016); however, these storage options provide only limited storage space. An alternative, underground H_2 storage (UHS), can store drastically more H_2, and can thus potentially be operated in a much more economical way. One example is H_2 storage in underground salt caverns—a method used for at least 30 years now (Tarkowski & Czapowski, 2018). Such salt caverns, however, are not abundant or geographically widespread. It is thus of high interest to evaluate additional geologic formations with respect to their H_2 storage potential (Pan et al., 2021). One target formation of interest are deep coal seams, which can adsorb and thus store substantial amounts of H_2 (Iglauer et al., 2021; Keshavarz et al., 2021). It is, however, vital that H_2 can be injected and withdrawn again in a fast, efficient manner. This essentially means that coal permeability must be sufficiently high so that H_2 gas flow is sufficiently rapid. This is for instance *not* the case for CO_2 geo-sequestration projects targeting coal seams, and it is well known that CO_2 injection leads to a dramatic loss of coal permeability due to coal swelling (e.g., Pan et al., 2010; Y. Zhang, Lebedev, et al., 2016). It is therefore of fundamental importance to examine coal swelling behavior when coal is exposed to pressurized H_2 gas, and how this is related to coal permeability.

We thus imaged H_2 gas injection into a coal core plug via high resolution in situ 3D x-ray micro-tomography (μCT) at true reservoir conditions, and measured how coal cleat morphology and the associated coal permeability changed due to H_2 exposure. This is presented and discussed in detail below.

Software: Adriana Paluszny
Supervision: Stefan Iglauer, Alireza
Keshavarz, Maxim Lebedev
Validation: Alireza Keshavarz
Visualization: Adriana Paluszny
Writing – original draft: Stefan Iglauer
Writing – review & editing: Alireza
Keshavarz, Muhammad Ali, Ausama
Giwelli, Lionel Esteban, Joel Sarout,
Maxim Lebedev

2. Experimental Procedure

A deep coal seam at a depth of approximately 250 m was simulated in the laboratory. Bituminous coal (from Morgantown, West Virginia, USA; supplied by Wards Scientific US; vitrinite reflectance = 0.86) was selected and small core plugs (5 mm diameter and 10 mm length) were drilled. The coal had a porosity of 3.7% (measured via Helium porosimetry using a CoreLab UltraPoroPerm-910 instrument), and the coal was also thoroughly analyzed via XRD (performed with a RAYONS X-Rays instrument equipped with a cobalt K_α radiation source at 40 kV and 40 mA), TGA (using a PerkinElmer-Thermogravimetric Analyzer-TGA 4000), ATR-FTIR (with a PerkinElmer-Spectrometer 100-FT-IR instrument), BET (performed at 77 K; to measure specific surface area, pore volume and average pore size of the coals using a Tristar II 3020 instrument) and ultimate and proximate analysis. Results are shown in Table 1 and in the Supporting Information.

The specific surface area of the coal was 0.34 m^2/g, average pore size was 16.38 nm, pore volume was 0.0014 cm^3/g and microporous content was 0.12. The mineral fraction in the coal consisted of 70 wt% quartz and 30 wt% kaolinite; ash composition was 46.5% SiO_2, 33.6% Al_2O_3, 10.9% Fe_2O_3, 2.04% CaO, 0.78 MgO, 1.52% Na_2O, 1.28% K_2O, 1.32% TiO_2, 0.02% Mn_3O_4, 0.17% P_2O_5, 1.09% SO_3, 0.29% SrO, 0.25% BaO, traces of ZnO and 0.05% V_2O_5. Furthermore, CO_2 and H_2 adsorption capacity and diffusion coefficients were measured previously (on separate coal samples) – demonstrating that substantial amounts of H_2 can be adsorbed (~0.1 mol H_2/kg coal at 3 MPa and 303 K) and that H_2 diffuses relatively quickly through the coal (a H_2 diffusion coefficient of ~1.5×10^{-8} m^2/s was measured for 296 K and 1.3 MPa equilibrium pressure), Iglauer et al. (2021); Keshavarz et al. (2021).

The coal plug was then placed into an x-ray transparent high pressure µCT cell (Iglauer & Lebedev, 2018) and vacuumed for 24 hr to remove all air from the system. The temperature was kept constant at 296 K (i.e., isothermal conditions), a pore pressure of 2.758 MPa was applied and overburden stress was raised to 6.205 MPa (i.e., 3.447 MPa effective stress was applied during the whole experiment), and the coal plug was µCT imaged at two high resolutions (1.50 and 4.00 µm, using the 3D x-ray microscope VersaXRM500 Xradia-Zeiss). Subsequently, 18,000 pore volumes H_2 gas (from BOC, HPG, 99.99 mol% purity) were injected into the plug applying a pressure drop of 0.22 MPa (2.978 MPa inlet pressure and 2.758 MPa outlet pressure). Three high precision syringe pumps (ISCO Teledyne 500D, accuracy 0.1%) were used to apply injection pressure, backpressure and overburden pressure with high accuracy. Dynamic coal permeability was measured during H_2-flooding by measuring the H_2 flow rate through the plug at this constant pressure drop and applying Darcy's law. H_2 injection was then stopped, and the system was kept at these conditions for 24 hr. The coal core was then µCT imaged again at the same high resolutions in-situ. Note that this µCT resolution is insufficient to resolve the complete pore space in the coal matrix, which can be even of atomic volume, but cleat (=fracture) networks can be reliably imaged (e.g., compare Ramandi et al., 2016; Y. Zhang, Lebedev, et al., 2016, Y. Zhang, Xu, et al., 2016).

The images were cropped, their image contrast adjusted, and outliers were removed via the application of a median filter, and the subsequent removal of outliers. The removal of outliers replaced a pixel by the median value of neighbors (radius of 2 pixels here), if the pixels was 50% brighter or darker than the neighborhood (Schneider et al., 2012). This process was performed for both bright and dark outliers three times, after which the percentage

Table 1
Proximate and Ultimate Analysis Results and Maceral Composition

Proximate analysis (wt %)					
	Inherent Moisture	Ash	Volatile Matter	Fixed Carbon	Carbonate Carbon
Bituminous	1.7	4.8	4.8	88.7	0.017
Ultimate analysis (wt %)					
	Carbon	Hydrogen	Nitrogen	Sulfur	Oxygen	Relative Density (%)
Bituminous	78.8	5.30	1.58	1.44	12.88	1.32
Maceral Composition (volumetric, %)					
	Vitrinite	Liptinite (Exinite)	Inertinite	Mineral Matter	Total Reactives	Vitrinite Reflectance
Bituminous	81.0	5.2	12.0	1.8	92.3	0.86
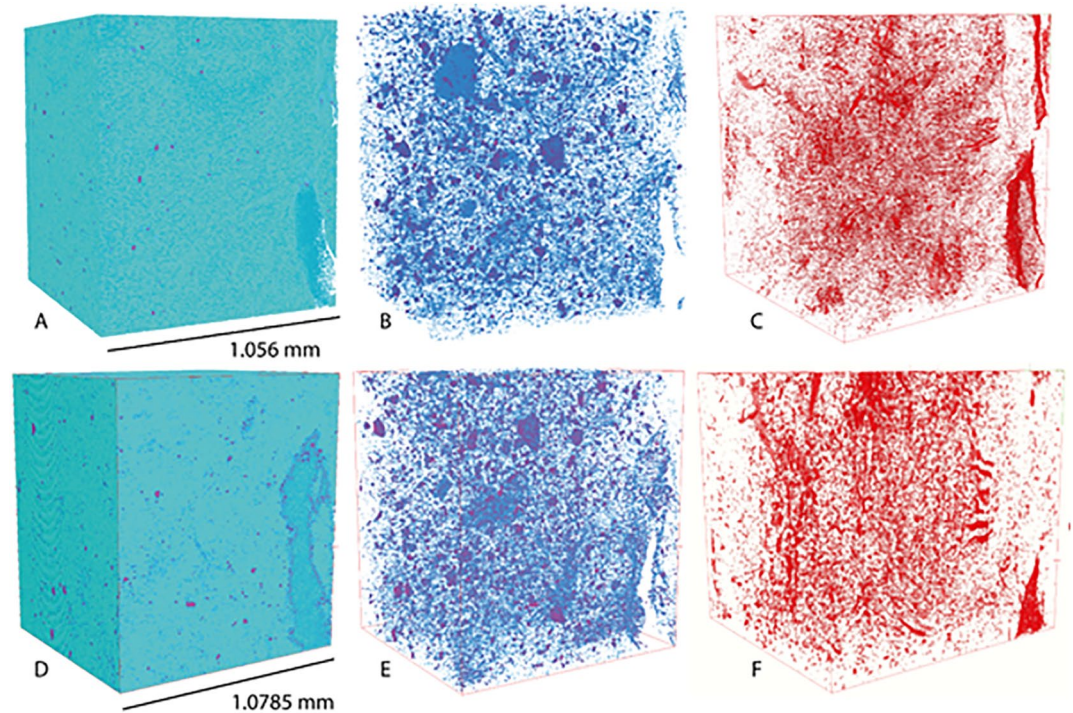
Figure 1. 3D visualizations of the coal phases before (top row) and after (bottom row) H_2-exposure. (a, d) maceral phase (turquoise); (b, e) mineral phase (blue); (c, f) cleats (=void space; red).

of removed outliers was below 5%. This conservative filtering was performed using Fiji ImageJ (Schindelin et al., 2012). The first and last 100 images were removed from the image stack to avoid the strongest ring artifacts. Darkest pixels were assumed to be void space as H_2 gas has a low x-ray attenuation. 3D void space (cleats) was segmented and counted in 3D using Fiji as well, taking into account integrated density, mean and standard deviation of gray values, minimum, maximum and average gray values, as well as computed centroids and centers of mass within the bounding box (Bolte & Cordelières, 2006).
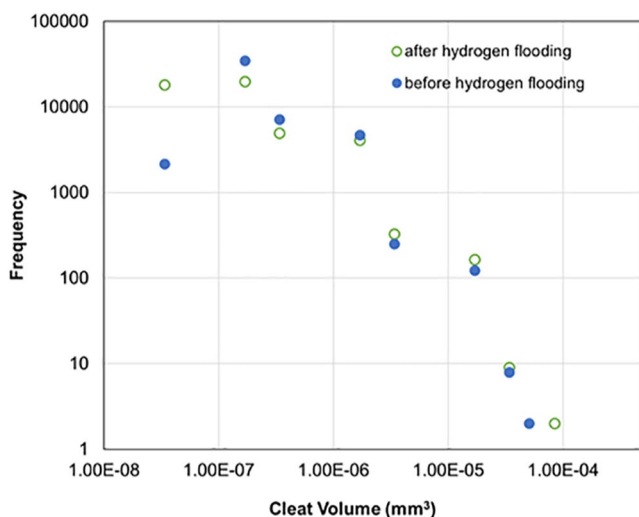
Figure 2. Cleat size distribution in the coal before and after H_2-flooding.

3. Results and Discussion

3.1. Coal Cleat Network Morphology Evolution

For H_2 geo-storage project assessment it is vital to know how much H_2 can be stored in a reasonable timeframe, and how fast H_2 can be withdrawn again (Pan et al., 2021). Previously, it has been shown that substantial amounts of H_2 can be adsorbed on the coal and storage capacity is thus in principle large (Iglauer et al., 2021). However, it is currently unknown how coal swelling and the associated coal permeability is affected by H_2-exposure; indeed, only very few data are available to assess UHS as a true economic technical option (Pan et al., 2021; F. Zhang, Zhao, et al., 2016). Potential changes in the coal cleat network characteristics (before and after H_2 flooding) were thus quantified and compared.

Importantly, H_2 exposure led to no measurable change in the coal cleat porosity, cleat network morphology or cleat size distribution (compare Figures 1 and 2 and Table 2 where the pore space morphology and the cleat network statistics before and after H_2 flooding are summarized). All phase fractions (mineral phase, maceral phase and the cleat system [void space]) remained constant during and after H_2-flooding, and fracture nucleation or propagation

Table 2
Coal Cleat Network Characteristics Before and After H_2 Flooding at 296 K, 2.758 MPa Pore Pressure and 3.447 MPa Effective Stress

Saturation state	Cleat porosity (%)[a]	Median cleat volume (mm³)[a]	Average cleat volume (mm³)[a]	Permeability (mD)
Before H_2 flooding	1.1	8.79×10^{-8}	18.8×10^{-8}	0.39
After H_2 flooding	1.1	5.07×10^{-8}	16.7×10^{-8}	0.39

[a]measured on the μCT images.

was not observed. Note that the small changes in Figures 1 and 2 and Table 2 were caused by the natural variation in coal (as the imaged volumes did not exactly overlap). We conclude that H_2 gas does not lead to swelling of the maceral phase; in contrast, CO_2 injection clearly leads to dramatic swelling of the maceral phase, even to the extent that the swelling stress is so high that it can fracture the mineral phase inside the coal (Y. Zhang, Lebedev, et al., 2016; Y. Zhang, Xu, et al., 2016). Compare these effects also with CH_4 and N_2 gas exposure; CH_4 exposure leads to significant maceral swelling, while N_2 exposure leads to minor maceral swelling (Zhou et al., 2013). Indeed, coal swelling follows the order $CO_2 > CH_4 > N_2 > H_2$. This is related to the polarizability of these molecules (and thus the Van der Waals interaction forces between the gas molecules and the maceral phase; CO_2 polarizability is 29.1×10^{-25} cm³, that of CH_4 is 25.9×10^{-25} cm³, that of N_2 is 17.4×10^{-25} cm³ and that of H_2 is 8×10^{-25} cm³; Ahmed & Rothenberger, 2015; Rallapalli et al., 2011), which directly determines maceral-gas interaction affinity, this is also for instance expressed in a much higher adsorption capacity of coal for CO_2 when compared to H_2 (Iglauer et al., 2021; Keshavarz et al., 2021). Note that CO_2 also forms hydrogen bonds with carbonyl and alcohol groups present in the coal, further increasing CO_2-coal affinity (Fujii et al., 2002).
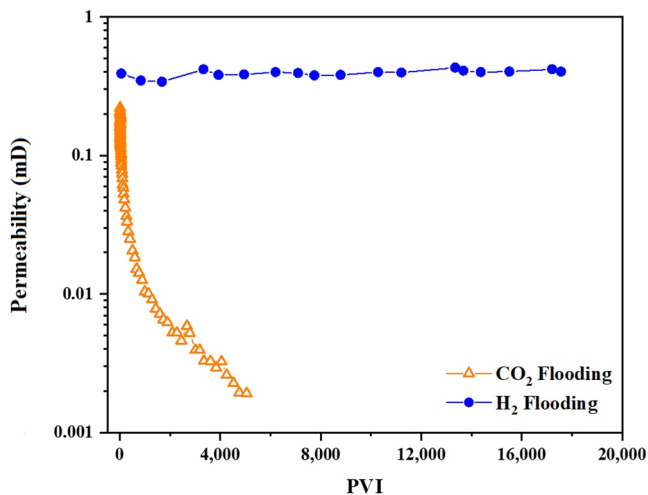
3.2. Dynamic Coal Permeability

Above observations are consistent with the measured dynamic coal permeability, which remained constant throughout H_2-flooding, Figure 3. The fluctuations were within the error margin of the experiment, and as can be seen permeability did not change even after flooding the core with 18,000 pore volumes of H_2. We conclude that injection of H_2 and subsequent withdrawal of H_2 from the storage reservoir is feasible from a fundamental fluid dynamical perspective. As high amounts of H_2 can be adsorbed, H_2 geo-storage in coal seams is a promising novel technique to store very large amounts of H_2 in a cost-effective manner.

4. Conclusions

H_2 geo-storage provides an alternative option for H_2 storage, at a giant scale (e.g., Tarkowski, 2019; F. Zhang, Zhao, et al., 2016). One key target formation are deep coal seams, which can adsorb large amounts of H_2 (Iglauer et al., 2021; Keshavarz et al., 2021; Pan et al., 2021). However, a sufficiently large coal permeability is required for efficient H_2 injection (for storage) and H_2 withdrawal (when the fuel is needed). In this context it is well known that CO_2 injection leads to dramatic swelling of the maceral (organic) phase, for example, Zhou et al. (2013); Y. Zhang, Lebedev, et al. (2016), which drastically reduces coal permeability. It is therefore of vital importance to assess how H_2-exposure influences the cleat network in the coal and the associated coal seam permeability. As this is unknown for H_2, we performed coal coreflooding tests and injected H_2 into a bituminous coal sample at UHS conditions (296 K, 2.758 MPa pore pressure, 3.447 MPa effective stress—which approximates the geothermal conditions prevailing at a depth of 250 m). The coal plug was imaged at high resolution with an x-ray tomograph, and coal permeability was measured in parallel. Importantly, no change in cleat morphology or permeability was observed.

We conclude that H_2-injection into deep coal seams does not induce coal swelling or permeability reduction—UHS in coal seams is thus feasible from a fundamental physico-chemical (high H_2 adsorption) and petro-physical (high injection and withdrawal rates are possible) perspective. This work therefore provides essential insights into coal permeability behavior when exposed to H_2 gas; and thus aids in the implementation of a large-scale hydrogen economy.

Figure 3. Dynamic coal permeability measured during H_2 flooding. PVI = pore volumes of H_2 injected.

Conflict of Interest

The authors declare no conflicts of interest relevant to this study.

Data Availability Statement

The data presented in this study are stored in the NERC EDS National Geoscience Data Centre (UK), and can be accessed here: https://www2.bgs.ac.uk/ngdc/citeddata/catalogue.html; https://www2.bgs.ac.uk/nationalgeo-sciencedatacentre/citedData/catalogue/84502681-f445-4a01-9dad-c561a94e7c87.html.

References

Ahmed, E., & Rothenberger, A. (2015). KFeSbTe$_3$: A quaternary chalcogenide aerogel for preferential adsorption of polarizable hydrocarbons and gases. *Journal of Materials Chemistry*, *3*, 7786–7792. https://doi.org/10.1039/c4ta06957a

Berta, M., Dethlefsen, F., Ebert, M., Schäfer, D., & Dahmke, A. (2018). Geochemical effects of millimolar hydrogen concentrations in groundwater: An experimental study in the context of subsurface hydrogen storage. *Environmental Science & Technology*, *52*(8), 4937–4949. https://doi.org/10.1021/acs.est.7b05467

Bolte, S., & Cordelières, F. P. (2006). A guided tour into subcellular colocalization analysis in light microscopy. *Journal of Microscopy*, *224*(3), 213–232. https://doi.org/10.1111/j.1365-2818.2006.01706.x

Fujii, A., Ebata, T., & Mikami, N. (2002). Direct observation of weak hydrogen bonds in microsolvated phenol: Infrared spectroscopy of O−H stretching vibrations of phenol-CO and -CO$_2$ in S0 and D0. *Journal of Physical Chemistry*, *106*, 10124–10129. https://doi.org/10.1021/jp0212601

Hanley, E. S., Deane, J. P., & O Gallachoir, B. P. (2018). The role of hydrogen in low carbon energy futures- a review of existing perspectives. *Renewable and Sustainable Energy Reviews*, *82*, 3027–3045. https://doi.org/10.1016/j.rser.2017.10.034

Iglauer, S., Abid, H., Al-Yaseri, A., & Keshavarz, A. (2021). Hydrogen adsorption on sub-bituminous coal: Implications for hydrogen geo-storage. *Geophysical Research Letters*, *48*(10), e2021GL092976. https://doi.org/10.1029/2021gl092976

Iglauer, S., & Lebedev, M. (2018). High pressure-elevated temperature x-ray micro-computed tomography for subsurface applications. *Advances in Colloid and Interface Science*, *256*, 393–410.

Keshavarz, A., Abid, H., Ali, M., & Iglauer, S. (2021). Hydrogen diffusion in coal: Implications for hydrogen geo-storage. *Journal of Colloid and Interface Science*, *608*, 1457–1462.

Pan, B., Yin, X., & Iglauer, S. (2021). Underground hydrogen storage: Influencing parameters and future outlook. *Advances in Colloid and Interface Science*, *294*, 102473. https://doi.org/10.1016/j.cis.2021.102473

Pan, Z., Conneell, L. D., & Camilleri, M. (2010). Laboratory characterisation of coal reservoir permeability for primary and enhanced coalbed methane recovery. *International Journal of Coal Geology*, *82*(3–4), 252–261. https://doi.org/10.1016/j.coal.2009.10.019

Rallapalli, P., Prasanth, K. P., Patil, D., Somani, R. S., Jasra, R. V., & Bajaj, H. C. (2011). Sorption studies of CO$_2$, CH$_4$, N$_2$, CO, O$_2$ and Ar on nanoporous aluminium terephthalate [MIL-53(Al)]. *Journal of Porous Materials*, *18*, 205–210. https://doi.org/10.1007/s10934-010-9371-7

Ramandi, H. L., Mostaghimi, P., Armstrong, R. T., Saadatfar, M., & Pinczewski, W. V. (2016). Porosity and permeability characterization of coal: A micro-computed tomography study. *International Journal of Coal Geology*, *154*, 57–68. https://doi.org/10.1016/j.coal.2015.10.001

Schindelin, J., Arganda-Carreras, I., Frise, E., Kaynig, V., Longair, M., Pietzsch, T., et al. (2012). Fiji: An open-source platform for biological-image analysis. *Nature Methods*, *9*, 676–682. https://doi.org/10.1038/nmeth.2019

Schneider, C., Rasband, W., & Eliceiri, K. (2012). NIH image to ImageJ: 25 years of image analysis. *Nature Methods*, *9*, 671–675. https://doi.org/10.1038/nmeth.2089

Tarkowski, R. (2019). Underground hydrogen storage: Characteristics and prospects. *Renewable and Sustainable Energy Reviews*, *105*, 86–94. https://doi.org/10.1016/j.rser.2019.01.051

Tarkowski, R., & Czapowski, G. (2018). Salt domes in Poland–potential sites for hydrogen storage in caverns. *International Journal of Hydrogen Energy*, *43*, 4621414–4621427. https://doi.org/10.1016/j.ijhydene.2018.09.212

Zhang, F., Zhao, P., Niu, M., & Maddy, J. (2016). The survey of key technologies in hydrogen energy storage. *International Journal of Hydrogen Energy*, *41*, 14535–14552. https://doi.org/10.1016/j.ijhydene.2016.05.293

Zhang, Y., Lebedev, M., Sarmadivaleh, M., Barifcani, A., & Iglauer, S. (2016). Swelling-induced changes in coal microstructure due to supercritical CO$_2$ injection. *Geophysical Research Letters*, *43*, 9077–9083. https://doi.org/10.1002/2016GL070654

Zhang, Y., Xu, X., Lebedev, M., Sarmadivaleh, M., Barifcani, A., & Iglauer, S. (2016). Multi-scale x-ray computed tomography analysis of coal microstructure and permeability changes as a function of effective stress. *International Journal of Coal Geology*, *165*, 149–156. https://doi.org/10.1016/j.coal.2016.08.016

Zhou, F., Hussain, F., Guo, Z., Yanici, S., & Cinar, Y. (2013). Adsorption/desorption characteristics for methane, nitrogen and carbon dioxide of coal samples from Southeast Qinshui Basin, China. *Energy Exploration & Exploitation*, *31*(4), 645–665. https://doi.org/10.1260/0144-5987.31.4.645